Eur. Phys. J. D (2017) 71: 289
DOI: 10.1140/epjd/e2017-80403-4

THE EUROPEAN PHYSICAL JOURNAL D

Regular Article

Electron transport in mercury vapor: cross sections, pressure and temperature dependence of transport coefficients and NDC effects*

Jasmina Mirić[1], Ilija Simonović[1], Zoran Lj. Petrović[1,2], Ronald D. White[3], and Saša Dujko[1,a]

[1] Institute of Physics, University of Belgrade, Pregrevica 118, 11080 Belgrade, Serbia
[2] Serbian Academy of Sciences and Arts, 11001 Belgrade, Serbia
[3] College of Science and Engineering, James Cook University, Townsville, QLD 4811, Australia

Received 13 June 2017 / Received in final form 15 September 2017
Published online 14 November 2017 – © EDP Sciences, Società Italiana di Fisica, Springer-Verlag 2017

Abstract. In this work we propose a complete and consistent set of cross sections for electron scattering in mercury vapor. The set is validated through a series of comparisons between swarm data calculated using a multi term theory for solving the Boltzmann equation and Monte Carlo simulations, and the available experimental data. Other sets of cross sections for electron scattering in mercury vapor were also used as input in our numerical codes with the aim of testing their completeness, consistency and accuracy. The calculated swarm parameters are compared with measurements in order to assess the quality of the cross sections in providing data for plasma modeling. In particular, we discuss the dependence of transport coefficients on the pressure and temperature of mercury vapor, and the occurrence of negative differential conductivity (NDC) in the limit of lower values of E/N. We have shown that the phenomenon of NDC is induced by the presence of mercury dimers and that can be controlled by varying either pressure or temperature of mercury vapor. The effective inelastic cross section for mercury dimers is estimated for a range of pressures and temperatures. It is shown that the measured and calculated drift velocities agree very well only if the effective inelastic cross section for mercury dimers and thermal motion of mercury atoms are carefully considered and implemented in numerical calculations.

1 Introduction

The behavior of electrons in mercury vapor under the influence of electric field is of vital interest in modeling of the gas-discharge lamps [1–3], lasers [4,5] and in special applications such as ion thrusters for space propulsion [6]. Further optimization and understanding of such applications is dependent on an accurate knowledge of the cross sections for electron scattering, transport coefficients and the physical processes involved. For example, fluid models of low-pressure discharges used in fluorescent lamps often require swarm transport parameters as a function of the reduced electric field and the gas temperature [7,8]. Current models of high-pressure mercury discharges, however, usually require a knowledge of the electrical conductivity, which can be calculated from the cross sections for electron scattering in mercury vapor and electron mobility.

A number of methods have been applied to investigate the behavior of electrons in mercury vapor and have been successfully applied to a variety of problems. For scattering theorists, the problem of the scattering of electrons on mercury atoms is challenging due to importance of relativistic effects and the correlation between different subshells which require the use of either Dirac equations or modified forms of the Schrödinger equation [9,10]. The correct representation of a very large low energy resonance in both elastic and momentum transfer cross sections below the first inelastic threshold of the $^3P_0$ state at 4.66 eV and impact of $6s6p^2$ resonances on the elastic scattering and the excitation cross-section in the energy range between 4 and 7 eV are also very important issues. This makes mercury a particularly interesting target for scattering theorists. No less challenging is the problem of the transport of electrons in mercury vapor, given the difficulties that occur in both the experimental measurements, as well as in theoretical calculations based on the Boltzmann equation and Monte Carlo simulations. For example, it is very difficult to find the experimental data in the literature for drift velocity and characteristic energy of electrons in mercury vapor for high values of the reduced electric fields, because such measurements require lower vapor pressure and therefore lower temperature, which is difficult to control accurately. In the domain of the theoretical studies of electron transport in the mercury

* Contribution to the Topical Issue "Physics of Ionized Gases (SPIG 2016)", edited by Goran Poparic, Bratislav Obradovic, Dragana Maric and Aleksandar Milosavljevic.

[a] e-mail: sasa.dujko@ipb.ac.rs

vapor based on the Boltzmann equation, only recently it has been shown that nonlocal effects, resonances and striations in mercury electrical discharges have much in common with the behavior of electrons in mercury vapor in the famous Franck–Hertz experiment [11–14].

In literature, already, some cross section sets for electron scattering in mercury vapor have been reported. Raju reviewed measured and theoretically calculated electron collision cross sections for mercury vapor and recommended the values of drift velocity and reduced ionization coefficient [15,16]. Complete sets of cross section were reported by Rockwood [17], Nakamura and Lucas [18,19], Sakai et al. [20] and Suzuki et al. [21]. Winkler et al. [22,23] and Yousfi et al. [24] made significant contributions to the development of transport and collision data for electrons in mercury vapors by including the kinetics of excited states and Penning ionization in their models of fluorescent lamps. The properties of electron swarms in pure mercury vapor have also been analyzed by Garamoon and Abdelhaleem [25], Braglia et al. [26] and Liu and Raju [27] while the effects of metastable mercury and argon atoms on electron transport were subject of studies performed by the group of Prof. Tagashira [20,28,29]. The influence of thermal motion of background mercury atoms on electron transport has been analyzed by Winkler et al. [30] while the impact of a magnetic field on various transport properties in a crossed field configuration was investigated by Liu and Raju [31].

The common thread among many of these previous studies is a systematic neglect of non-hydrodynamic behavior of transport coefficients, which is reflected in their dependence upon the pressure and temperature of mercury vapor. Moreover, the effects of thermal motion of mercury atoms have also been often neglected, duality of transport coefficients (e.g., the existence of two different families of transport coefficients, the bulk and the flux) for electrons in mercury vapor has never been considered and finally many studies have been made in the framework of the two term theory for solving the Boltzmann equation, despite its limitations and concerns regarding its accuracy that have been well-documented [32,33]. Using these facts as motivational factors, in this paper, we revisit the issue surrounding computation of electron transport properties in mercury vapor as a function of electric field, pressure and temperature of mercury vapor. As a first step, we have developed a complete set of cross sections for electron scattering in mercury vapor. We apply the standard swarm procedure of deriving cross sections [33–35]. The initial set of cross sections is composed of cross sections for the individual collision processes that are collected from the literature. Using this initial set of cross sections as an input for solving Boltzmann's equation, transport coefficients are calculated and compared with the corresponding experimental data. The initial cross sections are then modified and the procedure is repeated in order to obtain better agreement with the experimental transport coefficients. The cross sections are considered satisfactory when the calculated values for drift velocity, ionization coefficient and characteristic energy match the experimental values to within a standard experimental uncertainty.

Other sets of cross sections for electron scattering in mercury vapor that are available in the literature were also incorporated into the Boltzmann equation and Monte Carlo codes with the aim of assessing their completeness and accuracy. This has been done through a series of calculations focused on comparisons between the experimentally measured and theoretically calculated transport coefficients. In particular, we consider the pressure dependence of transport coefficients due to the presence of mercury dimers. The mercury dimers are molecular species that can cause a significant change in the rate of energy lost by the electrons via rotational and vibrational excitation and hence a considerable change in the drift velocity. The formation of dimers and their effect on the measured drift has been studied by Nakamura and Lucas [18,19], Elford [36] and England and Elford [37]. It was shown that the drift velocity increases with pressure, but the occurrence of negative differential conductivity (NDC) has not been reported. A cross section for momentum transfer in elastic collisions and an effective inelastic cross section for dimers have been derived using the well-established swarm method of deriving cross sections. In order to reduce the non-uniqueness of the initially derived cross section for momentum transfer, McEachran and Elford [10] have demonstrated that cross section for the momentum transfer can be further refined by considering the additional transport data.

In the present paper we extend the previous studies by considering the occurrence of NDC in the limit of lower values of E/N. NDC is the well-known phenomenon in transport theory which is characterized by a decrease in the drift velocity for increasing the applied electric field. The conditions for the occurrence of NDC have been investigated previously. It was shown that NDC can be induced and controlled by the presence of inelastic [38,39] and non-conservative collisions [40,41], electron–electron collisions [42,43] and anisotropic scattering [44]. For liquid argon and xenon, however, there is a new type of NDC that does not require inelastic collisions or non-conservative processes, i.e. it is purely a consequence of the medium structure [45,46]. In this work we demonstrate the NDC phenomenon induced by the presence of mercury dimers. The collision frequencies and the averaged energy losses due to elastic and inelastic collisions are calculated with the aim of explaining the development of NDC. The pressure dependence of other transport properties, including the mean energy and diffusion coefficients is also investigated. Particular attention is paid to the effects of the mercury vapor temperature and how this affects the basic properties of the drift and diffusion over a range of the reduced electric fields of practical interest. This has been done through a series of calculations based on a multi term theory for solving the Boltzmann equation and Monte Carlo simulation technique in which thermal motion of background mercury atoms is rigorously accounted for.

This paper is organized as follows. In Section 2 we outline the theory used to solve the Boltzmann equation and the basic elements of our Monte Carlo method for determining transport properties of electrons in mercury vapor. In Section 3.2 we present a new collision cross section set for electron scattering in mercury vapor, which revises the

previous sets summarized by Rockwood [17], Sakai et al. [20] and Suzuki et al. [21]. Comparison between the measured and calculated swarm data is shown in Section 3.3 while the pressure dependence of transport coefficients and dimer-induced negative differential conductivity are discussed in Section 3.4. In Section 3.5 we investigate the synergism of thermal effects and the effects induced by the mercury-dimers on electron transport in mercury vapor. Finally, we summarize our conclusions in Section 4 and also provide an outlook regarding the future transport studies for electrons in mercury vapor.

2 Methods of calculation

In this work, we investigate a swarm of electrons moving through a neutral gas under the influence of a uniform electric field. The electron number density is assumed to be sufficiently low so that the following conditions apply: (i) electron–electron interactions and space-charge effects can be neglected; (ii) the motion of the electrons can be treated classically, and (iii) the background of neutral atoms remains in thermal equilibrium. Electrons gain energy from the external electric field and dissipate it by collisions to the neutral gas atoms. The collisional transfer of this energy to the neutral gas atoms occurs by elastic and different types of inelastic collisions. This is a typical non-equilibrium system and its correct mathematical description can only be obtained from kinetic theory [47].

2.1 Multi term solution of Boltzmann's equation

To calculate the transport of electrons in mercury vapor, we apply a multi term solution of the Boltzmann equation for the phase-space distribution function $f(\mathbf{r},\mathbf{c},t)$:

$$\frac{\partial f}{\partial t}+\mathbf{c}\cdot\frac{\partial f}{\partial \mathbf{r}}+\frac{e\mathbf{E}}{m}\cdot\frac{\partial f}{\partial \mathbf{c}}=-J(f,f_0), \tag{1}$$

where $\mathbf{r}$ and $\mathbf{c}$ denote, respectively, the position and velocity co-ordinates in phase space, while e and m are the charge and mass of electron, respectively, and $\mathbf{E}$ is the applied external field. The right-hand side of equation (1) represents the collision operator J, describing the rate of change of the phase-space distribution function due to collisions between the electrons and the neutral background mercury vapor atoms.

In the present work we employ the original Boltzmann collision operator for elastic processes [48] and its semi-classical generalization for inelastic processes [49]:

$$J_{\rm in}(f,f_0)=\sum_{jk}\int\left[f(\mathbf{r},\mathbf{c},t)\,f_{0j}(\mathbf{c}_0)-f(\mathbf{r},\mathbf{c}',t)\,f_{0k}(\mathbf{c}_0')\right]\times g\sigma(jk;g,\widehat{\mathbf{g}}\cdot\widehat{\mathbf{g}}')\,d\widehat{\mathbf{g}}d\mathbf{c}_0, \tag{2}$$

where $\sigma(jk;g,\widehat{\mathbf{g}}\cdot\widehat{\mathbf{g}}')$ is the differential cross section for the scattering process $(j,\mathbf{c},\mathbf{c}_0)\rightarrow(k,\mathbf{c}',\mathbf{c}_0')$. This cross section depends on the electron's incident kinetic energy and on the angle between the incident and post-collision relative velocity, $\mathbf{g}$ and $\mathbf{g}'$, respectively. For a neutral mercury vapor with temperature T and number density N, the distribution of neutral velocities $\mathbf{c}_0$ in state j is Maxwell–Boltzmann:

$$f_0^{(j)}(\mathbf{c}_0)=\frac{N}{Z(T)}\exp\left(-\frac{\epsilon_j}{kT}\right)\omega(\alpha_0,\mathbf{c}_0), \tag{3}$$

where $Z(T)$ is the partition function, ϵ_j is the energy of a mercury atom (or mercury dimer) in quantum state j and

$$\omega(\alpha_0,\mathbf{c}_0)=\left(\frac{\alpha_0^2}{2\pi}\right)^{3/2}\exp\left(-\alpha_0^2c_0^2\right), \tag{4}$$

with $\alpha_0^2=m_0/kT$.

Electron ionization processes are described through the operator [51]:

$$J_I(f,f_0)=\sum_j N_{0j}c\big[\sigma_I(j;c)\,f(\mathbf{r},\mathbf{c},t)-2\times\int c'\sigma_I(j;c')\,B(\mathbf{c},\mathbf{c}';j)\,f(\mathbf{r},\mathbf{c}',t)\,d\mathbf{c}'\big], \tag{5}$$

where σ_I is the ionization cross section while $B(\mathbf{c},\mathbf{c}';j)$ is the probability for one of the two electrons after ionization having a velocity in the range $\mathbf{c}$ to $\mathbf{c}+d\mathbf{c}$, for incident electron velocity $\mathbf{c}'$, and N_{0j} is the number density of mercury atoms in the state j. In the present work we assume that all fractions are equally probable. The probability function must satisfy the following normalization conditions:

$$\int B(\mathbf{c},\mathbf{c}';j)\,d\mathbf{c}=1, \tag{6}$$

and

$$B(\mathbf{c},\mathbf{c}';j)=0,\qquad \text{if}\quad \epsilon'-\epsilon<\epsilon_I(j), \tag{7}$$

where ϵ' and ϵ are the incident and post-ionization energy of the electrons while $\epsilon_I(j)$ is the ionization potential of the jth channel.

Solution of non-conservative Boltzmann's equation (1) has been extensively discussed by Robson and Ness [50,51], White et al. [52,53] and Dujko et al. [54,55]. In brief, we expand the phase-space distribution function in terms of spherical harmonics with the aim of resolving its angular dependence in velocity space. Transport coefficients of charged particle swarms are exclusively defined in the hydrodynamic regime. In the hydrodynamic regime, the space-time dependence of the phase-space distribution function is expressed by an expansion in terms of the gradient of the electron number density $n(\mathbf{r},t)$. In order to resolve the speed-dependence of the phase-space distribution function, the expansion is made in terms of Sonine polynomials about a Maxwellian distribution function.

Thus, we solve equation (1) by making the expansions

$$f(\mathbf{r},\mathbf{c},t)=\omega(\alpha,c)\sum_{l=0}^{\infty}\sum_{m=-l}^{l}\sum_{\nu=0}^{\infty}\sum_{s=0}^{\infty}\sum_{\lambda=0}^{s}F(\nu lm|s\lambda)\times N_{\nu l}\left(\frac{\alpha c}{\sqrt{2}}\right)^{l}S_{l+1/2}^{(\nu)}\left(\frac{\alpha^2c^2}{2}\right)Y_m^{[l]}(\hat{\mathbf{c}})\,G_m^{(s\lambda)}n(\mathbf{r},t), \quad (8)$$

where $\omega(\alpha,c)$ is a Maxwellian distribution at a temperature T_b and $S_{l+1/2}^{(\nu)}\left(\frac{\alpha^2c^2}{2}\right)$ are Sonine polynomials. $Y_m^{[l]}(\hat{\mathbf{c}})$ is a spherical harmonic, a function of the angles $\hat{\mathbf{c}}$ and $G_m^{(s\lambda)}$ is the irreducible gradient tensor operator [50]. The two-term approximation which forms the basis of the conventional theories for solving the Boltzmann equation, is based upon the choice of setting the upper bound on the summation in (8) to $l_{\max}=1$. Its limitations and domains of applicability in calculating transport coefficients for electrons are thoroughly discussed in references [32,33].

Substitution of expansion (8) into equation (1) and performing the appropriate "matrix element" operations allows the Boltzmann equation to be converted into a set of matrix equations for the expansion coefficients $F(\nu lm|s\lambda)$,

$$\sum_{\nu'=0}^{\infty}\sum_{l'=0}^{\infty}\sum_{m'=-l'}^{l'}\left[M_{\nu lm,\,\nu'l'm'}+R\delta_{\nu'\nu}\delta_{l'l}\delta_{m'm}\right]\times F(\nu'l'm'|s\lambda)=X_{\nu lm}(s\lambda),\quad \nu,l=1,2,\ldots,\infty;\quad m=-l,\ldots,+l, \quad (9)$$

where R is the reaction rate. Explicit expressions for the matrix of coefficients $M_{\nu lm,\,\nu'l'm'}$, which contains the applied electric field and matrix elements of the collision operator, and right-hand side $X_{lm\nu}(s\lambda)$, can be found elsewhere [51,54]. The expansion coefficients $F(\nu lm|s\lambda)$ are called "moments" and are related to the electron transport properties as discussed in our previous works [52–55]. These quantities are numbers that depend on the applied electric field, the neutral number density N and cross sections for electron scattering. They are required for determination of both the bulk and the flux transport coefficients. The flux drift velocity is the swarm averaged velocity, while the bulk drift velocity is the rate of change of the swarm's centre of mass. The duality of transport coefficients and its implications in plasma modeling has been recently thoroughly discussed in references [56–59].

Of particular importance for the current paper is to note that the motion of the neutrals is systematically and rigorously incorporated into all collision process operators and all spherical harmonic equations. In contrast, in conventional theories which are usually based on the two term approximation, the consideration of the thermal motion of neutrals is often limited to the isotropic matrix elements of the elastic collision operator. Errors resulting from such theories will be discussed and illustrated in Section 3.4.

2.2 Monte Carlo method

A Monte Carlo simulation technique is also used in the present work, but as an independent tool with the aim of verifying the results of Boltzmann equation analysis. We follow the space and time development of a swarm of electrons in an infinite gas under the influence of a uniform electric field. The electron trajectories between collisions are determined by solving the collisionless equation of motion of a single electron. The position and velocity of each electron are updated after the time step Δt which is determined from the mean collision time divided by a large number (usually 100) depending on the simulation conditions. These small time steps Δt are used for numerical integration of the equation for the collision probability

$$p(t)=\nu_T(\epsilon(t))\exp\left(-\int_{t_0}^{t}\nu_T(\epsilon(t'))\,dt'\right), \quad (10)$$

where ν_T is the total collision frequency while t_0 is either the time of the electron entering the gas or the time of a previous collision. Equation (10) gives the probability that the electron will have a collision in the time interval $(t,t+dt)$ and its numerical solution requires the use of random numbers. The type of collision is also determined using random numbers as well as relative probabilities for individual collisional processes. The details of our Monte Carlo method and explicit formulas for both the bulk and flux transport coefficients are given in several of our previous publications [54,55,60–62].

Two important issues deserve more mentioning in this work. First, in our Monte Carlo code we have implemented the procedure for calculating the collision frequency in the case when thermal motion of the background gas cannot be neglected for a Maxwellian velocity distribution of the background gas particles. The details of the procedure can be found in the recent work of Ristivojević and Petrović [63]. This was a necessary step in this work, given the importance of thermal collisions for adequate description of electron transport in the limit of low electric fields.

Another issue in Monte Carlo simulations of electron transport in mercury vapor is the simulation speed. To achieve a good statistics of the final results and also to make sure that the relaxation of the steady-state conditions has been achieved, one needs to follow a large number of electrons. Due to numerous elastic collisions in which only a fraction of the initial electron energy is transferred to a heavy mercury atom target, the efficiency of energy transfer between the electrons and neutral mercury atoms is very low. As a consequence, the relaxation of energy is a very slow process and requires large computation time. In order to optimize the simulation speed, the simulations were usually began with a relatively low number of electrons (typically 1.5×10^3) and after relaxation to the steady state the electron swarm was scaled up in numbers at fixed time intervals. The newly created electron has the same dynamic properties as the original one until the first collision. Following the first collision the progeny and the original electrons follow different, independent trajectories. Detailed testing has shown that this technique does not affect the final results, but speeds up

the relaxation considerably. For more details the reader is referred to [54].

3 Results and discussion

3.1 Preliminaries

In the first part of this section we cover a range of reduced electric fields between 0.1 and 1000 Td. The temperature of the mercury vapor is 293 K while the pressure is set to 1 Torr. Under these conditions the impact of mercury dimers is negligible. In what follows these conditions will be designated as "no dimers". In the second part of the present work, we consider a much narrower range of the reduced electric fields: 0.1–3 Td. The temperature is set to 573 K and calculations are performed for a range of pressures. The influence of mercury dimers on the drift velocity and other transport properties is investigated over a range of conditions that are consistent with those present in the experiment of England and Elford [37]. In the last segment of this work, the transport coefficients are calculated using our new set of cross sections for electron scattering in mercury vapor over a range of E/N values and temperatures relevant to light sources which utilize mercury discharges.

The transport coefficients shown below are functions of E/N and are expressed using the unit of Townsend ($1\ \mathrm{Td} = 10^{-21}\ \mathrm{Vm}^2$). Calculations are performed assuming that the internal states are governed by a Maxwell–Boltzmann distribution which essentially places all mercury atoms in the ground state. All scattering is assumed isotropic and hence elastic cross section is the same as the elastic momentum transfer cross section. The thermal motion of background particles is carefully considered in both Boltzmann equation analysis and in Monte Carlo simulations.

3.2 Cross sections for electron scattering in mercury vapor

In this work, we consider electron transport in mercury vapor using the cross section set developed in this study. This set of cross sections is shown in Figure 1. The cross section for momentum transfer in elastic collisions is made as follows. For lower electron energies, we use the experimentally derived cross section of England and Elford [37] while for higher energies, we use a cross section tabulated in MAGBOLTZ code [64]. As discussed by England and Elford, care must be taken in deriving of a cross section for momentum transfer from the measured drift velocities due to diffusion effects and the presence of mercury dimers [37]. Cross sections for electronic excitations for levels $^3P_0$, $^3P_1$ and $^3P_2$ are retrieved from [65] while electronic excitations to $^1S_0$ and $^1P_1$ states as well as a cross section for higher states are also taken from MAGBOLTZ code. For electron-impact ionization, we have used the cross section from [66]. Cross sections were slightly modified during the calculations to improve agreement between the calculated and measured swarm parameters. We found that we were able to achieve a good agreement between calculated and measured drift velocities for lower E/N by adjusting only the magnitude of the elastic momentum transfer cross section. For higher E/N (e.g. for higher electron energies), we have slightly modified the cross sections for electronic excitations in order to reproduce the measured ionization coefficient. This procedure is based on the experience that the calculated ionization rate is affected more by the modifications of the cross sections for electronic excitations than by the modifications of the ionization cross section [33,35].

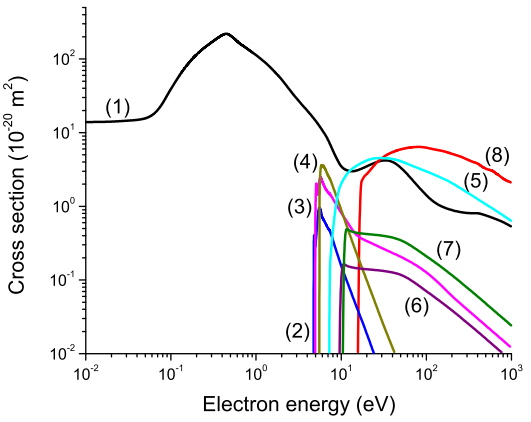

Fig. 1. Cross sections for electron scattering in Hg vapor: (1) elastic momentum transfer, (2) excitation $^3P_0$, (3) excitation $^3P_1$, (4) excitation $^3P_2$, (5) excitation $^1P_1$, (6) excitation $^1S_0$, (7) excitation to higher states and (8) ionization.

A single effective inelastic cross section with the energy threshold of 0.04 eV is added to our cross section set, for electron scattering on mercury atoms, in order to represent the energy losses and momentum changes due to rotational and vibrational excitations of mercury dimers. It was necessary to include an effective cross section, since there are no cross sections for other channels of electron scattering on mercury dimers in the literature. There are no competing processes in the same energy range for collisions on monomers thus the contribution of the rotational–vibrational excitation will be significant. In principle, we may assume that the abundance of the dimers is sufficiently low so their overall contribution is negligible for processes that have a competing channel in scattering on monomer. In other words, we may assume that for all the other processes the cross sections are the same as for the monomer and we may apply an effective cross section for rotational and vibrational excitation of dimers and add that process to the set of cross sections for monomers. This effective cross section is derived using the experimental measurements of Elford and co-workers [36,37]. We have used the following assumptions:

- mercury dimers are always present in mercury vapor at a concentration proportional to the number density of mercury atoms;
- in order to account for the dimer number density, the amplitude of the effective cross section is scaled with their fractional abundance;
- the ideal gas law is assumed for the equation of state of mercury vapor.

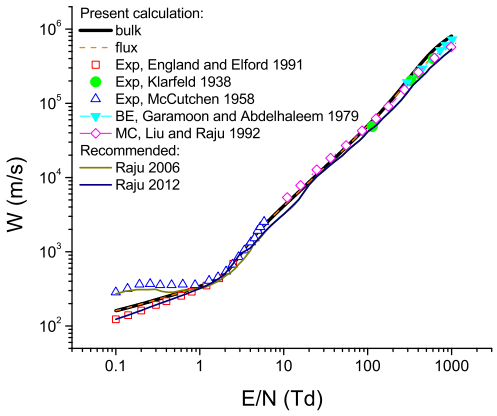

Fig. 2. Comparison of the drift velocity calculated using the present set of cross sections with the available experimental measurements of England and Elford [37], Klarfeld [67] and McCutchen [68]. Our results for the drift velocity are also compared with the available Monte Carlo calculations [27], Boltzmann equation results [25] and with the data recommended by Raju [15,16].

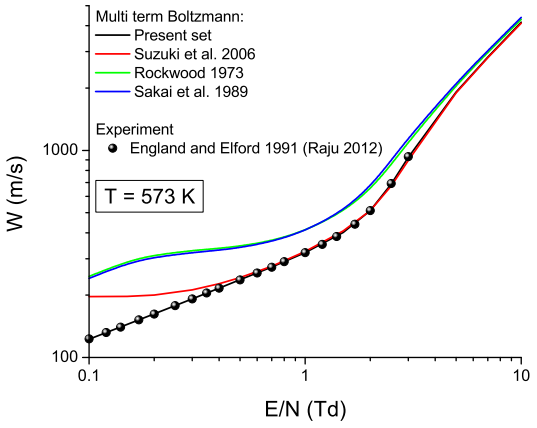

Fig. 3. Comparison of the drift velocity calculated using the present set of cross sections with those calculated using the cross sections sets developed by Rockwood [17], Sakai et al. [20] and Suzuki et al. [21]. Results are presented for the lower values of E/N and are compared with the measurements of England and Elford [37] which have been recommended by Raju [16]. The temperature of the dimer-free mercury vapor is 573 K.

The effective cross section for dimers at pressure p and temperature T is given by [37]

$$\sigma(\epsilon) = 8.3\,\sigma_i(\epsilon)\,\Delta(p,T), \tag{11}$$

where 8.3 is a maximal value of the cross section at fractional dimer abundance of 1 ppm, $\sigma_i(\epsilon)$ is the dimer cross section used to fit the measurements of drift velocity and $\Delta(p,T)$ is the fractional abundance of dimers at pressure p and temperature T. Cross sections $\sigma_i(\epsilon)$ as a function of electron energy in units of squared angstroms are given by England and Elford [37]. Using the above assumptions and a value of 21.8×10^{-6} for fractional abundance of dimers at the pressure of 1 kPa and temperature of 573 K we have

$$\frac{\Delta(p,T)}{\Delta_1(p_1,T_1)} = \frac{n}{n_1} = \frac{p}{p_1}\frac{T_1}{T}, \tag{12}$$

and hence

$$\Delta(p,T) = 21.8 \times 10^{-6}\,\frac{p}{1\text{ kPa}}\,\frac{573\text{ K}}{T}. \tag{13}$$

Combining equations (11) and (13) yields the following simple expression for deriving the dimer cross section at the pressure p and temperature T

$$\sigma(\epsilon) = 180 \times 10^{-6}\,\frac{p}{1\text{ kPa}}\,\frac{573\text{ K}}{T}\,\sigma_i(\epsilon). \tag{14}$$

From equation (14) it is clear that the mercury-dimer cross section depends on the ratio p/T. If the mercury vapor temperature T is fixed and the pressure p is increased, then the mercury-dimer cross section grows and vice versa, if one keeps the pressure p fixed and increases the mercury vapor temperature T, then the mercury-dimer cross section declines. However, it should be noted that the saturated mercury vapor pressure at 573 K is 33 kPa (approximately 248 Torr). This means that at the temperature of 573 K it is not possible to consider the influence of pressures higher than 33 kPa, and vice versa, it is not possible to consider the transport of electrons at a pressure of 33 kPa for the temperature less than 573 K. These conditions correspond to liquid mercury, which is certainly beyond the scope of this work.

The effective cross section which describes rotational and vibrational excitations of mercury dimers is considerable at higher pressures and lower temperatures. The corresponding superelastic cross section has been calculated using the principle of detailed balance in a thermal equilibrium.

3.3 Comparison between measured and calculated transport coefficients

In order to test the present set of cross sections for electron scattering in mercury vapor, we compare our theoretically calculated transport coefficients with various measurements and other calculations under conditions in which the influence of mercury dimers is negligible. In particular, we compare our calculations with the two sets of data recommended and published by Raju [15,16]. The transport coefficients are shown in Figures 2–6 as functions of E/N. Calculations are performed using the present set of cross sections and those developed by Rockwood [17], Sakai et al. [20] and Suzuki et al. [21]. We have applied a multi term approach for solving the Boltzmann equation assuming the pressure of 1 Torr while the temperature of mercury vapor is set to 293 K. Under these conditions the influence of mercury dimers on transport coefficients could be neglected. The convergence of transport coefficients was good and a value of $l_{\max} = 5$ was generally required for achieving an accuracy to within 1% or better.

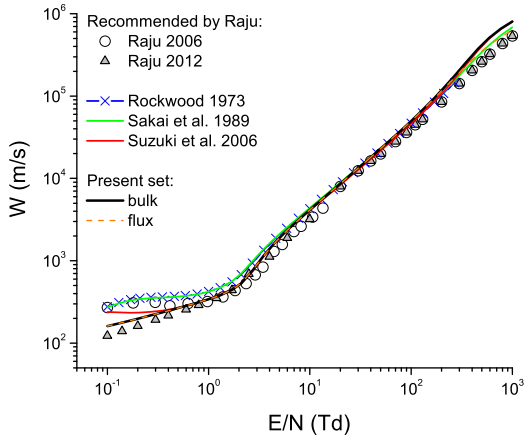

Fig. 4. Comparison of the drift velocity calculated using the present set of cross sections with those calculated using the cross sections sets developed by Rockwood [17], Sakai et al. [20] and Suzuki et al. [21]. Results are also compared with the drift velocity data recommended by Raju [15,16]. The temperature of the dimer-free mercury vapor is 293 K.

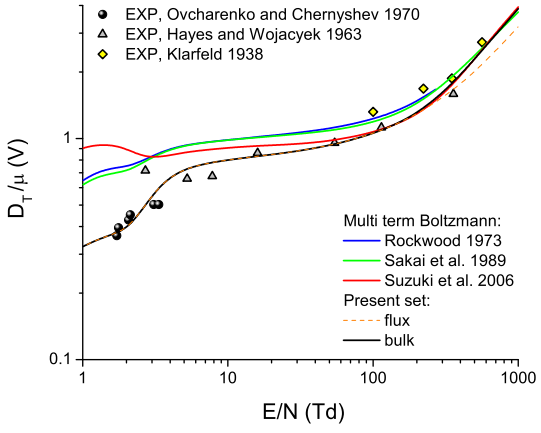

Fig. 5. Comparison of the characteristic energy, calculated using the present set of cross sections with those calculated using the cross section sets developed by Rockwood [17], Sakai et al. [20] and Suzuki et al. [21]. Results are also compared with the measurements of Ovcharenko and Chernyshev [69], Hayes and Wojacyek [70] and Klarfeld [67].

The bulk and flux drift velocities along with the experimental results of Klarfeld [67], McCutchen [68] and those recommended by Raju [15,16] are shown in Figure 2. The values of drift velocity calculated by a Monte Carlo simulation technique [27] and those obtained by solving the Boltzmann equation [25] are also plotted. For the low values of E/N we observe relatively poor agreement between our results and measurements of England and Elford [37]. This follows from the fact that our calculations have been performed assuming the mercury vapor temperature of 293 K while the experimental values of drift velocities in a dimer-free mercury vapor of England and Elford are obtained at 573 K. The Raju's 2012 recommended data are consistent with the measurements England and Elford [37]. After increasing the temperature of dimer-free mercury vapor to 573 K in our calculations, we have observed

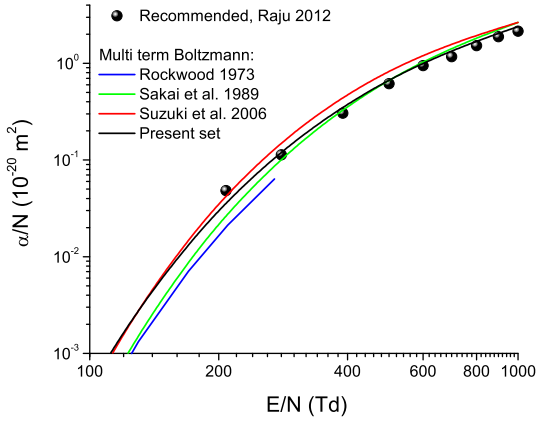

Fig. 6. Comparison of the ionization coefficient calculated using the present set of cross sections with those calculated using the cross section sets developed by Rockwood [17], Sakai et al. [20] and Suzuki et al. [21]. Results are also compared with the Raju's 2012 recommended data.

an excellent agreement between the calculated and measured drift velocities (see Fig. 3). Comparing our results and those measured by McCutchen [68], it is evident that a significant disagreement exists (see Fig. 2). The signs of NDC are clearly evident in the measurements of McCutchen [68]. This suggests that the experiment was operated under conditions in which the traces of mercury dimers were present. Indeed, the pressure of mercury vapor in his experiment was set to 350 Torr while no temperatures were given for any experimental runs. The agreement between our results and measurements of McCutchen [68] becomes much better for the higher values of E/N as the impact of mercury dimers on the drift velocity is reduced. At intermediate fields (10 Td$<$ E/N $<$100 Td), our results and Monte Carlo results of Liu and Raju [27] agree also very well. At higher E/N, above 100 Td, we see that the present calculations tend to lie a little above the experimental results of Klarfeld [67] and calculations of Garamoon and Abdelhaleem [25]. Nevertheless, the agreement is still quite reasonable. Due to the explicit contribution of ionization, the differences between the bulk and flux values of the drift velocity are of the order of 25% in the limit of the highest E/N considered in this work. Below 100 Td, however there is no appreciable difference between the two. In conclusion, from the profile of the drift velocity calculated using the present set of cross sections and temperature of 293 K for mercury vapor, there are no signs of NDC, i.e., the drift velocity is a monotonically increasing function of E/N.

In Figure 4 we show the variation of the flux and bulk drift velocities with E/N. The plots were calculated using the present set of cross sections and those developed by Rockwood [17], Sakai et al. [20] and Suzuki et al. [21]. For clarity, the flux drift velocity is shown only for the present set of cross sections. The results are also compared with the two sets of Raju's recommended data [15,16]. For the lower values of E/N, we again observe the inconsistency between our calculated data assuming the present set of cross sections and Raju's 2012 recommended data [16]. Increasing the temperature of the

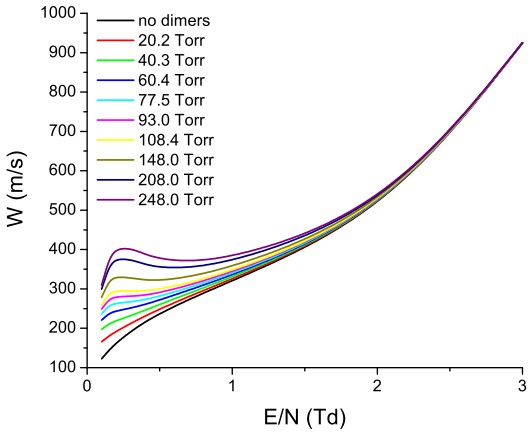

Fig. 7. Drift velocity as a function of E/N for a range of pressures. The temperature of the mercury vapor is 573 K.

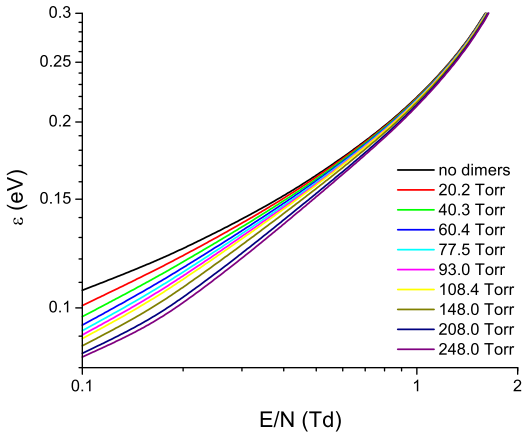

Fig. 8. Mean energy as a function of E/N for the same conditions as in Figure 7.

mercury vapor to 573 K the agreement between our calculations and Raju's 2012 recommended data is excellent (see Fig. 3). In the same region of E/N, the agreement between the calculated drift velocities assuming the cross section sets developed by Rockwood [17] and Sakai et al. [20] is very good. The agreement is not surprising, since the cross section for momentum transfer in elastic collisions developed by Rockwood [17] was also used by Sakai et al. [20]. For the intermediate values of E/N (10 Td< E/N <100 Td), we observe the excellent agreement between all calculated drift velocities. For the higher values of E/N, the agreement is slightly deteriorated. The calculated flux drift velocity using the present set of cross sections agrees reasonably well with the calculated bulk drift velocity assuming the set of cross sections developed by Sakai et al. [20]. On the other hand, the bulk drift velocities calculated using the present set and a set of cross sections developed by Suzuki et al. [21] agree very well. The set of cross sections developed by Rockwood [17] could not be used for calculations in the limit of higher E/N since it covers the range of electron energies only up to 30 eV. In conclusion, with the exception of the Raju's 2006 recommended data, our calculations clearly show the absence of NDC for all sets of cross sections employed in this work.

Figure 5 shows the flux and the bulk characteristic energies as a function of E/N. The characteristic energy provides a good estimate of the average energy of the electrons in the swarm. This quantity is extremely sensitive to the presence of inelastic processes and hence its comparison with experimental data indicates the quality of the energy balance of the cross section sets under consideration. Calculations using the present set of cross sections and those developed by Rockwood [17], Sakai et al. [20] and Suzuki et al. [21] are compared with the experimental results of Ovcharenko and Chernyshev [69], Hayes and Wojacyek [70] and Klarfeld [67]. For the lower values of E/N, we observe that the characteristic energy calculated from the present set of cross sections is in quite nice agreement with measurements of Ovcharenko and Chernyshev [69]. The agreement is also good with the measurements of Hayes and Wojacyek [70] for the intermediate values of E/N while in the limit of the highest E/N considered in this work, the calculated values approach to each other and generally tend to lie a little below the experimental results of Klarfeld [67].

In Figure 6 we show the variation of the ionization coefficient with E/N. Calculations using the present set of cross sections and those published by Rockwood [17], Sakai et al. [20] and Suzuki et al. [21] are compared with the Raju's 2012 recommended data. The agreement between Raju's 2012 recommended data and those calculated assuming the present set of cross sections is very good. On the other hand, calculations assuming the set of cross sections developed by Suzuki et al. [21] are systematically higher than Raju's 2012 recommended data while calculations using the sets of cross sections developed by Rockwood [17] and Sakai et al. [20] are lower at low E/N than Raju's 2012 recommended data. We observe that calculation based on the present set of cross sections slightly deviate from the Raju's 2012 recommended data only in the limit of lower E/N. One may expect such behavior as the computer code must cope with very small values of the distribution function in the energy region where the ionization cross section is appreciable. Furthermore, the experimental measurements of the ionization coefficient in the vicinity of the ionization threshold, usually have great uncertainty.

3.4 Pressure dependence of transport coefficients and NDC effect

In this section we investigate the effects of mercury dimes on electron transport. Calculations are performed for a range of pressures while the temperature of mercury vapor is set to 573 K. The cross sections detailed in Section 3.2 and displayed in Figure 1 are used as an input into Monte Carlo simulations. In Figure 7 we show the drift velocity as a function of E/N for a range of pressures. From Figure 7 we see that the drift velocity increases with the pressure of mercury vapor for low values of E/N and becomes pressure independent for higher values of E/N. Other transport coefficients and properties show pressure

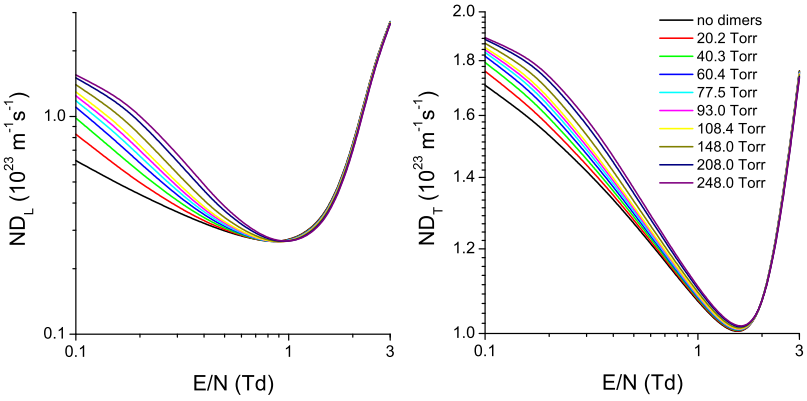

Fig. 9. Longitudinal and transverse diffusion coefficients as a function of E/N for the same conditions as in Figure 7.

dependence over the same range of E/N. As an illustrative example, in Figures 8 and 9 we show the variation of the mean energy and diffusion coefficients with E/N. While the mean energy decreases with an increasing pressure, the diffusion coefficients are increased. The pressure dependence of the drift velocity (and other transport coefficients) arises through the pressure dependence of the dimer cross section. It is well known that in elastic collisions a fraction of the initial energy m/M is transferred from the electron to the neutral particle, while for inelastic collisions a considerably larger fixed energy loss is transferred in addition, per each interaction. Assuming isotropic model of scattering, the vector of electron velocity is arbitrarily oriented after collisions, which leads to a reduction in the directed component of the velocity. In other words, elastic collisions have the effect of randomizing the direction of electron motion, while preserving their speeds. When inelastic collisions are significant, however, the energy transfer is no longer relatively small. This in turns reduces the chaotic component of the electron velocity, and inelastic collisions no longer have the effect of randomizing the direction of electron motion. This indicates that the increase in gas pressure enhances drift velocity and reduces mean energy. For higher electron energies, the cross section for mercury dimers is reduced and transport coefficients become pressure independent.

In addition to the pressure dependence of the drift velocity and other transport coefficients, we observe the presence of NDC in the profiles of drift velocity in the limit of pressures that approach to the pressure of saturated mercury vapor. A study of the NDC for model gases was performed by Petrović et al. [38] in which the conditions for elastic and inelastic cross sections required for the occurrence of NDC were discussed. Using momentum transfer theory, Robson had developed an analytical criterion for NDC in a conservative single gas [39] that was further extended in [40]. An intimate connection between NDC and inelastic collisions was recognized in these studies. It was shown that NDC arises for certain combinations of elastic and inelastic cross sections in which, on increasing the electric field, there is a rapid transition from inelastic to elastic dominated energy loss mechanism. In this transition region, for a given increase in the electric field, a greater proportion of the energy input goes into chaotic motion rather than directed motion. As a consequence, the drift velocity falls with an increasing electric field.

This is exactly what happens in mercury vapor at higher pressures. As already discussed, mercury dimers are always present in a mercury vapor at a concentration proportional to the vapor pressure. Thus, as the pressure of mercury vapor increases, the dimer cross section increases as well as the corresponding collision frequency (see Fig. 10). For pressures higher than approximately 100 Torr and in the limit of lower values of E/N, the inelastic energy loss mechanism dominates the elastic energy loss mechanism. For increasing E/N the collision frequency of inelastic collisions decreases while the collision frequency for elastic collisions rises. This favors the development of NDC even though the difference between the collision frequencies is almost five orders of magnitude! However, if one takes into account that the average energy loss in an elastic collision is between 1×10^{-7} and 1×10^{-6} eV, while the energy loss in inelastic collisions is 0.04 eV, it is clear that a relatively small ratio between collision frequencies in inelastic and elastic collisions is compensated by the substantial differences in energy losses. At pressures lower than approximately 100 Torr, the concentration of mercury dimers is low. As a consequence, the energy losses in inelastic collisions are significantly lower than those in elastic collisions over the entire range of E/N. Under these conditions, NDC does not occur in the E/N profiles of the drift velocity.

These physical arguments are illustrated in Figure 11. Figure 11 shows the ratio between the average elastic and inelastic energy losses as a function of E/N. The average inelastic energy loss Ω_{inel} is evaluated as a product of the rate coefficient for an inelastic dimer process and the corresponding threshold of 0.04 eV. It should be noted that the elastic energy loss Ω_{elas} is approximated by the product of mean energy, the collision frequency of elastic collisions and the factor $2m/M$. By doing so, we have actually reduced the contribution of elastic collisions, having in mind that the collision frequency of elastic collisions and the corresponding energy losses are greater for electrons with energies higher than the average electron energy. The accurate calculation may be very efficiently performed in Monte Carlo simulations, but we defer this to a future

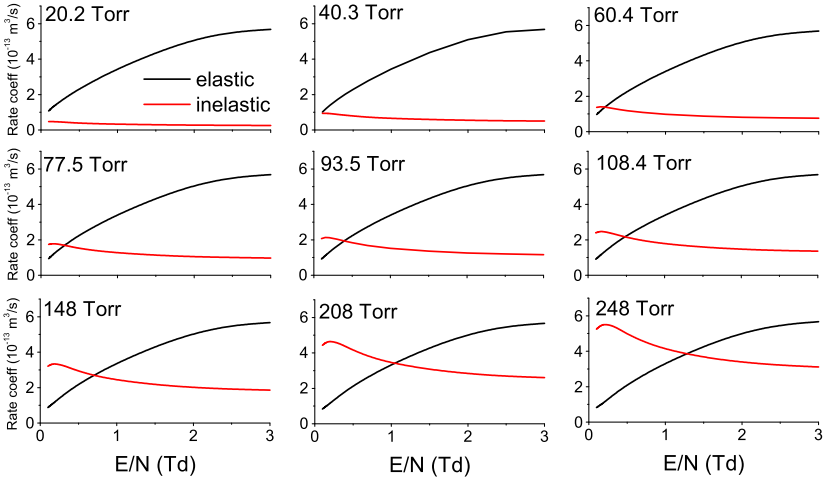

Fig. 10. Rate coefficients for elastic and inelastic collisions as a function of E/N in the presence of mercury dimers. The rate coefficient of inelastic processes which describes the presence of dimers is multiplied by the factor of 1×10^5. Calculations are performed for the same conditions as in Figure 7.

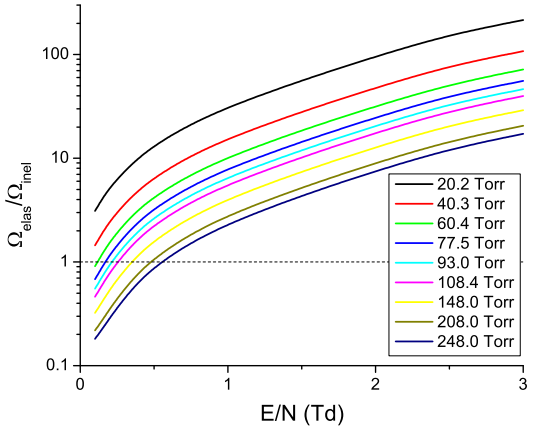

Fig. 11. Ratio between the average elastic and inelastic energy losses as a function of E/N for the same conditions as in Figure 7.

work. In any case, we observe that only for higher pressures of mercury vapor the ratio between energy losses in elastic and inelastic collisions favors the development of NDC.

Figures 12 and 13 illustrate the importance of including an accurate representation for thermal motion of the mercury atoms in our analysis of the drift velocity in the limit of lower values of E/N. Our multi term Boltzmann equation results with the rigorously incorporated effects of thermal motion of the mercury atoms are compared with our Monte Carlo results obtained under the conditions in which no thermal motion is considered. Our Monte Carlo results with the systematically incorporated effects of thermal motion of the mercury atoms are not included in this figure as they are essentially the same as those obtained through a multi term approach for solving the Boltzmann equation. Both sets of our calculated data are compared with the measurements of England and Elford [37]. Comparing experiment and our Boltzmann equation results with the rigorously incorporated effects of thermal motion of the mercury atoms, we observe an excellent agreement between these two sets of data. In contrast, our Monte Carlo simulation results in which no thermal motion of the mercury atoms is considered, systematically overestimate the measurements in the limit of the lowest E/N. A false NDC like structure in the Monte Carlo $T = 0$ profiles of the drift velocity for all pressures of the mercury vapor is clearly evident. However, for increasing E/N the agreement between the measurements and Monte Carlo simulations in which no thermal motion is considered, becomes much better. As expected, the disagreement between the measurements and Monte Carlo simulations in which no thermal motion is considered is more pronounced for higher pressures.

3.5 Temperature dependence of transport coefficients

In this section we present results showing the variation of transport properties with E/N and mercury vapor temperature, T. Calculations are performed for two different cases: (1) the presence of mercury dimers assuming the pressure of 248 Torr, and (2) no dimers in the mercury vapor. Temperatures less than 573 K cannot be considered in the first scenario as for this pressure the mercury is in liquid form. These two scenarios for our calculations are considered with the aim of separating the thermal effects from those induced by mercury dimers.

In Figure 14 we show the variation of the mean energy with E/N for various mercury vapor temperatures, T. We observe that the mean energy is a monotonically increasing function of E/N for a fixed T. In the limit of low values of E/N the mean energy of the electrons is thermal and does not depend on E/N. This suggests that the velocity distribution function is essentially a thermal Maxwellian. For increasing T, the thermal deadlock is broken at higher E/N. For $T = 573$ K and $T = 1000$ K, we observe that the mean energy is higher in the case where

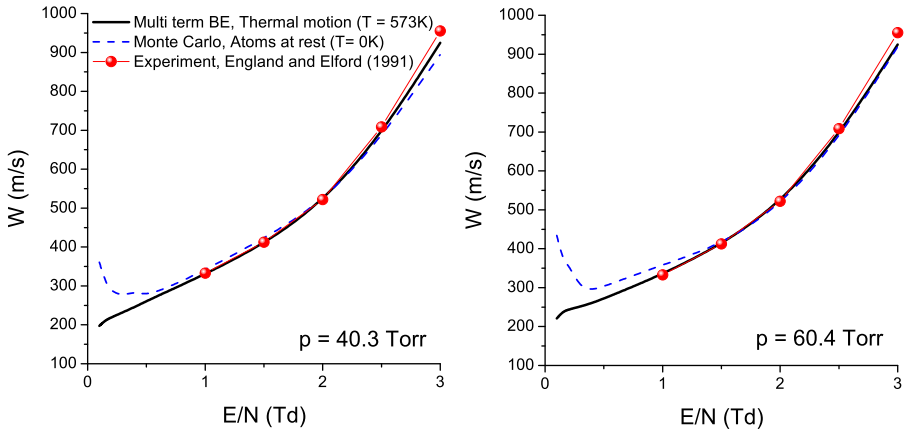

Fig. 12. Comparison between the calculated and measured values of drift velocity for pressures of 40.3 Torr (left panel) and 60.4 Torr (right panel). Monte Carlo results are obtained assuming atoms at rest ($T = 0$ K) while the gas temperature effects are considered through a multi term approach for solving the Boltzmann equation ($T = 573$ K).

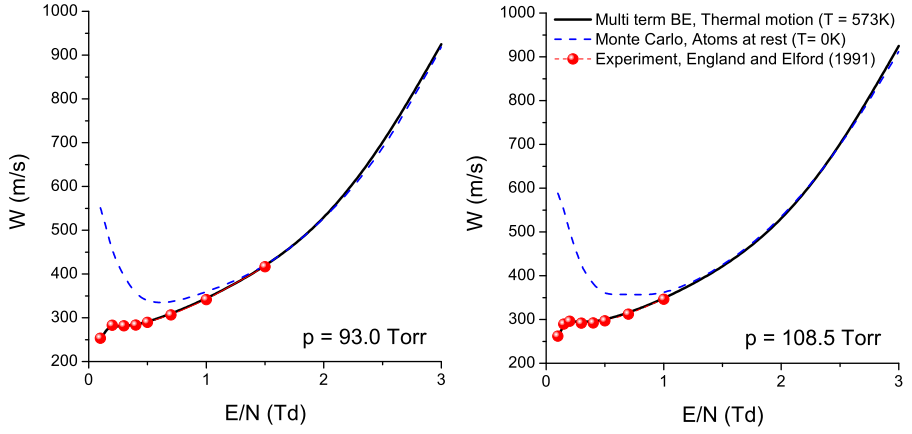

Fig. 13. Comparison between the calculated and measured values of drift velocity for pressures of 93.0 Torr (left panel) and 108.5 Torr (right panel). Calculations are performed for the same conditions as in Figure 12.

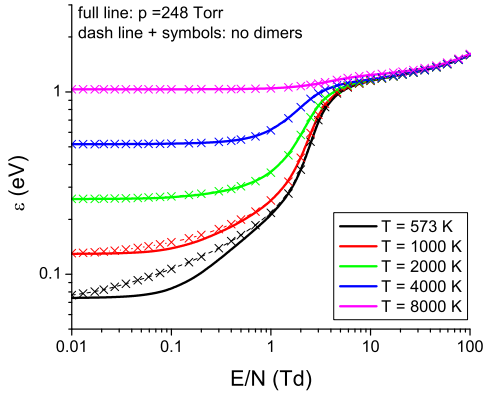

Fig. 14. Variation of the mean energy of the electron swarm as a function of E/N for various mercury vapor temperatures as indicated on the graph. The pressure of mercury vapor is 248 Torr.

no mercury dimers occur. It is clear that when the mercury dimers are present, the electrons lose more energy in inelastic collisions. For $T \geq 2000$ K the influence of mercury dimers is negligible. For low and intermediate values of E/N the mean energy is distinctively dependent on T. In the limit of higher values of E/N the mean energies are higher than the corresponding thermal mean energies, which is a clear sign that the velocity distribution function is no longer a thermal Maxwellian. In this regime, the impact of the mercury vapor temperature T on the mean energies is minimal.

In Figures 15 and 16 we show the variation of the drift velocity with E/N for various mercury vapor temperatures, T. The drift velocity is a monotonically increasing function of E/N for all mercury vapor temperatures T, except for $T = 573$ K. At this temperature, NDC is clearly evident in the E/N-profile of drift velocity. With further increase in mercury vapor temperature, a decrease in drift velocity with increasing E/N is firstly reduced and then it is completely removed. From equation (14) it is clear that for increasing mercury vapor temperature and fixed pressure, the mercury-dimer cross section declines. As a consequence, the collision frequency of inelastic collisions whose presence is of an essential importance for the development of NDC effect, is also firstly reduced, and then severely minimized which ultimately leads to a disappearance of

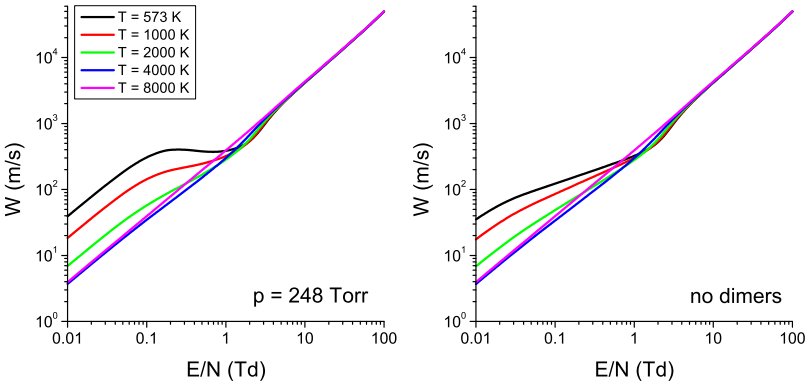

Fig. 15. Variation of the bulk drift velocity of the electron swarm as a function of E/N for the same conditions as in Figure 14.

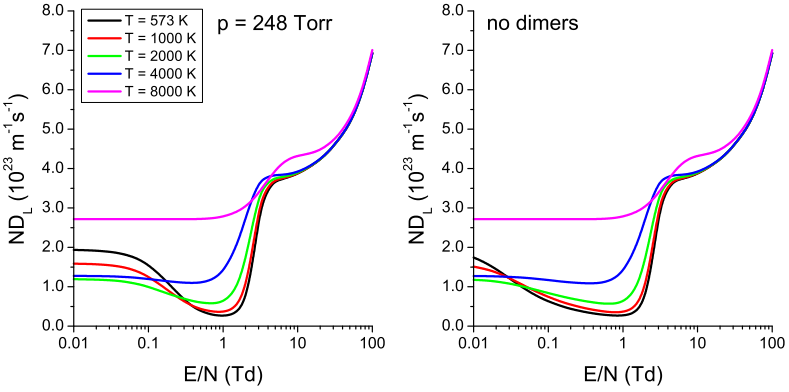

Fig. 16. Variation of the bulk longitudinal diffusion coefficient of the electron swarm as a function of E/N for the same conditions as in Figure 14.

NDC. The lesson from this is that the temperature of mercury vapor can be used to control the occurrence of NDC.

In the limit of lower E/N the drift velocity generally decreases with increasing T, though this is not the case for $T = 8000$ K. For $T = 8000$ K we see that the drift velocity is above the values calculated for $T = 4000$ K. For the temperature of 8000 K, the mean energy is high enough to exceed the peak value of the "0.4 eV" shape resonance in the cross section for elastic scattering. On the other hand, for $T = 4000$ K, the mean energy is significantly lower and corresponds to the range of energies in which the cross section for elastic collisions rises with an increasing energy of the electrons. As a consequence, the drift velocity is lower. For the intermediate values of E/N (between 1 and 10 Td, approximately) the behavior of drift velocity is very complex. In the energy region corresponding to the intermediate values of E/N, there is an overlap of the distribution function not only with a very large resonance in the elastic cross section, but also with the cross sections of inelastic processes that are now open. Finally, for higher values of E/N the drift velocity does not depend on the mercury vapor temperature and the drift of the electrons is entirely controlled by the electric field.

The variation of the diffusion coefficients with E/N for various mercury vapor temperatures, T, is shown in Figures 16 and 17. The impact of mercury dimers on both ND_L and ND_T is evident only for lower values of E/N and lower T. At fixed T and for increasing E/N the electric field rises the energy of the electrons and the mercury-dimer cross section begins to fall. The same occurs at fixed E/N and with increasing T. Furthermore, in the limit of the lowest E/N and for a fixed E/N both ND_L and ND_T display a minimum with respect to T. In contrast to the drift velocity, the minimum occurs at $T = 2000$ K, indicating that diffusion coefficients show a remarkable sensitivity to the energy dependence of cross sections and presence of inelastic collisions. For the intermediate values of E/N, the most distinct property is the existence of a local minimum in the E/N profiles of both ND_L and ND_T. With a decreasing temperature, the minimum becomes more pronounced and is shifted towards higher E/N. The fall in both ND_L and ND_T by increasing E/N reflects the rapidly rising elastic cross section, e.g., the velocity distribution function samples the lower energy branch of the "0.4 eV" shape resonance. Comparing the behavior of diffusion coefficients at low and intermediate values of E/N, one can see that the contribution of mercury dimers is more important for lower values of E/N. In the limit of higher E/N, the impact of temperature on the behavior of diffusion coefficients is minimal. However, the longitudinal diffusion coefficient shows a more complex behavior with varying temperature.

In Figure 18 we show variation of the ratio ND_T to ND_L with E/N for various mercury vapor temperatures,

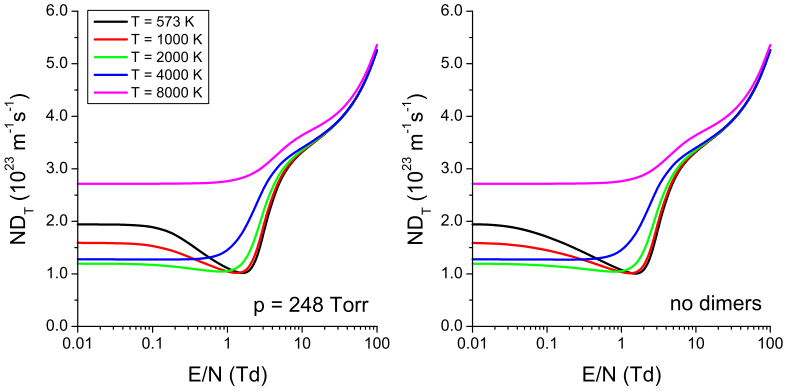

Fig. 17. Variation of the bulk transverse diffusion coefficient of the electron swarm as a function of E/N for the same conditions as in Figure 14.

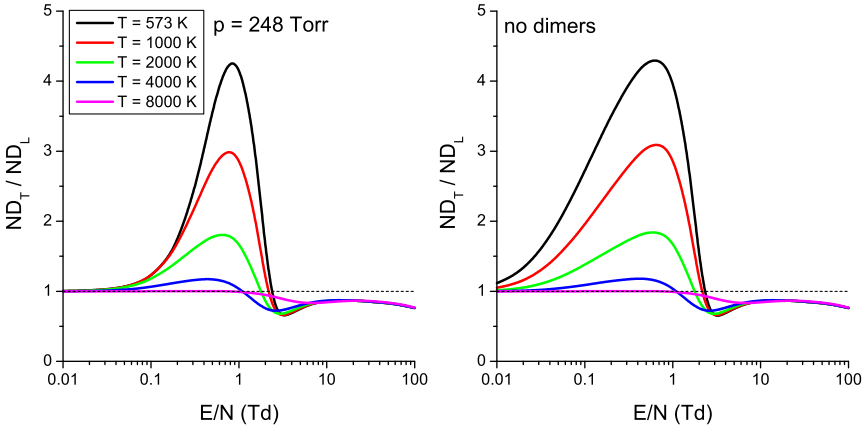

Fig. 18. Variation of the ratio of transverse to longitudinal diffusion coefficient of the electron swarm as a function of E/N for the same conditions as in Figure 14. Bulk values of diffusion coefficients are used.

T. We observe that the degree of anisotropic diffusion is significantly reduced by increasing mercury vapor temperature, T, in both scenarios considered here, i.e., in the presence of dimers and in their absence. In the limit of the lowest E/N diffusion is isotropic, i.e. $ND_L = ND_T$ since velocity distribution function is a thermal Maxwellian. At a fixed T the ratio ND_T/ND_L increases with increasing E/N, reaching a maximal value between 0.5 and 0.9 Td depending on the temperature T, and then it starts to decrease with E/N. For $T = 573$ K there is a factor higher than 4 between the longitudinal and transverse diffusion coefficients. In contrast, for $T = 8000$ K the diffusion is isotropic in a wide range of E/N, and only for $E/N > 1$ Td, the longitudinal diffusion coefficient is greater than the transverse, i.e. $ND_L > ND_T$. The reversal of the inequality is a clear sign of the rapid fall in the elastic cross section. Indeed, in this energy range the velocity distribution function samples the high energy branch of the "0.4" shape resonance of the elastic cross sections which rapidly falls with increasing electron energy.

4 Conclusion

In this paper, we have presented the results of a systematic investigation of electron transport in mercury vapor under the influence of electric field. First, we have compiled a complete set of cross sections for electron scattering in mercury vapor using the available data in the literature for individual collisional processes. In our evaluation, performed both with multi term Boltzmann and Monte Carlo codes, the initially compiled set of cross sections has been modified in order to reproduce the experimental data. The best agreement between calculated and measured drift velocities in the limit of lower electron energies was achieved by adjusting only the magnitude of the elastic momentum transfer cross section. For higher electron energies, we have only slightly modified the cross sections for electronic excitations in order to reproduce the measured ionization coefficient. We have also considered the issue of assessing the completeness, accuracy, and consistency of other cross section sets for electron scattering in mercury vapor by comparing calculated transport coefficients with those measured in various experiments. Our calculations highlight some inadequacies in these sets of cross sections and indicate possibilities for their improvements.

We have also outlined issues associated with the pressure and temperature dependences of transport coefficients. It was shown that the pressure dependence of the transport coefficients arise through the pressure dependence of the mercury-dimer cross section. In particular,

we have discussed the NDC phenomenon in the limit of lower values of the reduced electric fields. Conditions leading to NDC have been discussed and it was concluded that the phenomenon is induced by the presence of mercury dimers. Following the previous works of England and Elford [37], we have derived the mercury-dimer cross section for a range of pressures and temperatures of mercury vapor. One of the critical elements in our analysis of the drift velocity in the limit of lower values of the reduced electric fields was an accurate representation for thermal motion of the mercury atoms. Within a multi term theory for solving the Boltzmann equation used in the present work, the thermal motion of the neutral mercury atoms is systematically incorporated into all collision process operators and all spherical harmonic equations. Likewise, our Monte Carlo simulation code has been improved by implementing an efficient algorithm for calculating the collision frequency in the case when thermal motion of the background gas cannot be neglected for a Maxwellian velocity distribution of the background gas particles. Without these critical elements in a theory for solving the Boltzmann equation and Monte Carlo simulation codes, the variation of the drift velocity with the reduced electric field is unphysical in domain of lower electric fields.

Using a set of cross sections presented in this work, in the near future we plan to investigate the electron transport in crossed electric and magnetic fields. Calculations will be made with the aim of providing the data for fluid modeling of inductively coupled mercury discharges which are utilized in some types of electrodeless lamps. Similar calculations will be performed for ac electric and magnetic fields having in mind that both the electric and magnetic fields could be time-dependent. We also plan to develop complete and consistent sets of cross section for other materials, including indium, sodium and other metal vapors relevant for the lighting industry. The first steps have been made and the results are very encouraging [71].

This work was supported by the Grant Nos. ON171037 and III41011 from the Ministry of Education, Science and Technological Development of the Republic of Serbia and also by the project 155 of the Serbian Academy of Sciences and Arts. RDW acknowledges support from the Australian Research Council.

Author contribution statement

All authors contributed equally to the paper.

References

1. G.G. Lister, J.E. Lawler, W.P. Lapatovich, V.A. Godyak, Rev. Mod. Phys. **76**, 541 (2004)
2. P. Flesch, *Light and light sources* (Springer, Berlin, 2006)
3. S. Samukawa, M. Hori, S. Rauf, K. Tachibana, P. Bruggeman, G. Kroesen, J.C. Whitehead, A.B. Murphy, A.F. Gutso, S. Starikovskaia, U. Kortshagen, J.P. Boeuf, T.J. Sommerer, M.J. Kushner, U. Czarnetzki, N. Mason, J. Phys. D: Appl. Phys. **45**, 25300 (2012)
4. G.J. Fetzer, J.J. Rocca, IEEE J. Quantum Electron. **28**, 1941 (1992)
5. C.E. Little, *Metal vapour lasers: physics, engineering and applications* (Wiley, Chichester, 1999)
6. E. Ahedo, Plasma Phys. Control. Fusion **53**, 124037 (2011)
7. G.G. Lister, J.J. Curry, J.E. Lawler, J. Phys. D: Appl. Phys. **37**, 3099 (2004)
8. W.J.M. Brok, M.F. Gendre, M. Haverlag, J.J.A.M. van der Mullen, J. Phys. D: Appl. Phys. **40**, 3931 (2007)
9. O. Zatsarinny, K. Bartschat, Phys. Rev. A **79**, 042713 (2009)
10. R.P. McEachran, M.T. Elford, J. Phys. B: At. Mol. Opt. Phys. **36**, 427 (2003)
11. R.E. Robson, R.D. White, M. Hildebrandt, Eur. Phys. J. D **68**, 188 (2014)
12. Y. Golubovskii, S. Gorchakov, D. Uhrlandt, Plasma Sources Sci. Technol. **22**, 023001 (2013)
13. F. Sigeneger, R. Winkler, R.E. Robson, Contrib. Plasma Phys. **43**, 178 (2003)
14. R.E. Robson, B. Li, R.D. White, J. Phys. B: At. Mol. Opt. Phys. **33**, 507 (2000)
15. G.G. Raju, *Gaseous electronics: theory and practice* (CRC Press Taylor & Francis, Boca Raton, 2006)
16. G.G. Raju, *Gaseous electronics: tables, atoms, and molecules* (CRC Press Taylor & Francis, Boca Raton, 2012)
17. S.D. Rockwood, Phys. Rev. A **8**, 2348 (1973)
18. Y. Nakamura, J. Lucas, J. Phys. D: Appl. Phys. **11**, 325 (1978)
19. Y. Nakamura, J. Lucas, J. Phys. D: Appl. Phys. **11**, 337 (1978)
20. Y. Sakai, S. Sawada, H. Tagashira, J. Phys. D: Appl. Phys. **22**, 276 (1989)
21. S. Suzuki, K. Kuzuma, H. Itoh, J. Plasma Fusion Res. Series **7**, 314 (2006)
22. R.B. Winkler, J. Wilhelm, R. Winkler, Ann. Phys. (Leipz.) **40**, 90 (1983)
23. R.B. Winkler, J. Wilhelm, R. Winkler, Ann. Phys. (Leipz.) **40**, 119 (1983)
24. M. Yousfi, G. Zissis, A. Alkaa, J.J. Damelincourt, Phys. Rev. A **42**, 978 (1990)
25. A.A. Garamoon, A.S. Abdelhaleem, J. Phys. D: Appl. Phys. **12**, 2181 (1979)
26. G.L. Braglia, M. Diligenti, J. Wilhelm, R. Winkler, Il Nuevo Cimento **12**, 257 (1990)
27. J. Liu, G.R. Govinda Raju, J. Phys. D: Appl. Phys. **25**, 167 (1992)
28. S. Sawada, Y. Sakai, H. Tagashira, J. Phys. D: Appl. Phys. **22**, 282 (1989)
29. Y. Sakai, S. Sawada, H. Tagashira, J. Phys. D: Appl. Phys. **24**, 283 (1991)
30. R. Winkler, J. Wilhelm, G.L. Braglia, M. Diligenti, Il Nuevo Cimento **12**, 975 (1990)
31. J. Liu, G.R. Govinda Raju, J. Phys. D: Appl. Phys. **25**, 465 (1992)
32. R.D. White, R.E. Robson, B. Schmidt, M.A. Morrison, J. Phys. D: Appl. Phys. **36**, 3125 (2003)
33. Z.Lj. Petrović, S. Dujko, D. Marić, G. Malović, Ž. Nikitović, O. Šašić, J. Jovanović, V. Stojanović, M. Radmilović-Radjenović, J. Phys. D: Appl. Phys. **42**, 194002 (2009)
34. L.G.H. Huxley, R.W. Crompton, *The drift and diffusion of electrons in gases* (Wiley, New York, 1974)
35. Z.Lj. Petrović, M. Šuvakov, Ž. Nikitović, S. Dujko, O. Šašić, J. Jovanović, G. Malović, V. Stojanović, Plasma Sources Sci. Technol. **16**, S1 (2007)

36. M.T. Elford, Aust. J. Phys. **33**, 231 (1980)
37. J.P. England, M.T. Elford, Aust. J. Phys. **44**, 647 (1991)
38. Z.Lj. Petrović, R.W. Crompton, G.N. Haddad, Aust. J. Phys. **37**, 23 (1984)
39. R.E. Robson, Aust. J. Phys. **37**, 35 (1984)
40. S.B. Vrhovac, Z.Lj. Petrović, Phys. Rev. E **53**, 4012 (1996)
41. J. Mirić, D. Bošnjaković, I. Simonović, Z.Lj. Petrović, S. Dujko, Plasma Sources Sci. Technol. **25**, 065010 (2016)
42. N.L. Aleksandrov, N.A. Dyatko, I.V. Kochetov, A.P. Napartovich, D. Lo, Phys. Rev. E **53**, 2730 (1996)
43. Z. Donko, N. Dyatko, Eur. Phys. J. D **70**, 135 (2016)
44. K. Yamamoto, N. Ikuta, J. Phys. Soc. Jpn. **68**, 2602 (1999)
45. G.J. Boyle, R.P. McEachran, D.G. Cocks, R.D. White, J. Chem. Phys. **142**, 154507 (2015)
46. G.J. Boyle, D.G. Cocks, R.P. McEachran, M.J. Brunger, S.J. Buckman, S. Dujko, R.D. White, J. Phys. D: Appl. Phys. **49**, 355201 (2016)
47. F. Taccogna, G. Dilecce, Eur. Phys. J. D **70**, 251 (2016)
48. L. Boltzmann, Wein. Ber. **66**, 275 (1872)
49. C.S. Wang-Chang, G.E. Uhlenbeck, J. DeBoer, in *Studies in statistical mechanics*, edited by J. DeBoer, G.E. Uhlenbeck (Wiley, New York, 1964), Vol. 2, p. 241
50. R.E. Robson, K.F. Ness, Phys. Rev. A **33**, 2068 (1986)
51. K.F. Ness, R.E. Robson, Phys. Rev. A **34**, 2185 (1986)
52. R.D. White, K.F. Ness, R.E. Robson, Appl. Surf. Sci. **192**, 26 (2002)
53. R.D. White, R.E. Robson, S. Dujko, P. Nicoletopoulos, B. Li, J. Phys. D: Appl. Phys. **42**, 194001 (2009)
54. S. Dujko, R.D. White, Z.Lj. Petrović, R.E. Robson, Phys. Rev. E **81**, 046403 (2010)
55. S. Dujko, R.D. White, Z.Lj. Petrović, R.E. Robson, Plasma Source Sci. Technol. **20**, 024013 (2011)
56. R.E. Robson, R.D. White, Z.Lj. Petrović, Rev. Mod. Phys. **77**, 1303 (2005)
57. S. Dujko, A.H. Markosyan, R.D. White, U. Ebert, J. Phys. D: Appl. Phys. **46**, 475202 (2013)
58. A.H. Markosyan, S. Dujko, U. Ebert, J. Phys. D: Appl. Phys. **46**, 475203 (2013)
59. D. Bošnjaković, Z.Lj. Petrović, S. Dujko, J. Phys. D: Appl. Phys. **49**, 405201 (2016)
60. Z.Lj. Petrović, Z.M. Raspopović, S. Dujko, T. Makabe, Appl. Surf. Sci. **192**, 1 (2002)
61. S. Dujko, Z.M. Raspopović, Z.Lj. Petrović, J. Phys. D: Appl. Phys. **38**, 2952 (2005)
62. S. Dujko, R.D. White, Z.Lj. Petrović, J. Phys. D: Appl. Phys. **41**, 245205 (2008)
63. Z. Ristivojević, Z.Lj. Petrović, Plasma Sources Sci. Technol. **21**, 035001 (2012)
64. http://magboltz.web.cern.ch/magboltz
65. K. Bartschat, *Third Int. Conf. on Atomic and Molecular Data and their Applications* (American Institute of Physics, New York, 2003)
66. J. Kieffer, G.H. Dunn, Rev. Mod. Phys. **38**, 1 (1966)
67. B. Klarfeld, Tech. Phys. (USSR) **5**, 913 (1938)
68. C.W. McCutchen, Phys. Rev. **112**, 1848 (1958)
69. V.A. Ovcharenko, S.M. Chernyshev, Teplofiz. Vys. Temp. **8**, 716 (1970)
70. E. Hayes, K. Wojacyek, Beitr. Plasma Phys. **3**, 74 (1963)
71. J. Mirić, Z.Lj. Petrović, R.D. White, S. Dujko, *Proc. 27th Summer School and Int. Symp. on the Physics of Ionized Gases (Belgrade)* (Institute of Physics, Belgrade, 2014), p. 126